formed using the CHILL radar through the cooperation of the Universities of Chicago and Illinois, and are reported by Al-Khatib *et al.* [11]. A cooperative research program with the Appleton Laboratory, England, using the Chilbolton 10-cm radar facility has also been initiated to investigate the signal properties of horizontally and vertically polarized waves under various switching conditions [10]. These studies are expected to provide additional insights on the technique and on the meteorological interpretation of data derived from radars equipped to measure Z_{DR}.

ACKNOWLEDGMENT

The authors are grateful to Dr. R. C. Srivastava of the University of Chicago, IL, and Dr. E. A. Mueller of the Illinois State Water Survey for their encouragement and support in the use of the CHILL Radar Facility.

REFERENCES

[1] T. A. Seliga, and V. N. Bringi, "Potential use of radar differential reflectivity measurements at orthogonal polarizations for measuring precipitation," *J. Appl. Meteor.*, vol. 15, pp. 69–76, 1976.
[2] —, "Differential reflectivity and differential phase shift: Applications in radar meteorology," *Radio Sci.*, vol. 13, pp. 271–275, 1978.
[3] A. Hendry, and G. C. McCormick, "Polarization properties of precipitation particles related to storm structure," *J. Rech. Atmos.*, vol. 8, pp. 189–200, 1974.
[4] H. R. Pruppacher, and K. V. Beard, "A wind tunnel investigation of the internal circulation and shape of water drops falling at terminal velocity in air," *Quart. J. Roy. Meteor. Soc.*, vol. 96, pp. 247–256, 1970.
[5] A. W. Green, "An approximation for the shapes of large raindrops," *J. Appl. Meteor.*, vol. 14, pp. 1578–1583, 1975.
[6] R. Gunn, and G. D. Kinzer, "The terminal velocity of fall for water droplets in stagnant air," *J. Meteor.*, vol. 6, pp. 243–248, 1949.
[7] C. W. Ulbrich, and D. Atlas, "The rain parameter diagram: Methods and applications," *J. Geophys. Res.*, vol. 83, pp. 1319–1325, 1978.
[8] G. C. McCormick, and A. Hendry, "Principles for the radar determination of the polarization properties of precipitation," *Radio Sci.*, vol. 10, pp. 421–434, 1975.
[9] L. J. Battan, *Radar Observation of the Atmosphere.* Chicago, IL: Univ. Chicago Press, 1973, p. 324.
[10] V. N. Bringi, S. M. Cherry, M. P. M. Hall, and T. A. Seliga, "A new accuracy in determining rainfall rates and attenuation due to rain by means of dual-polarization radar measurements," in *Proc. IEE Int. Conf. Antenna and Propagat.*, pp. 120–124, Nov. 1978.
[11] H. H. Al-Khatib, T. A. Seliga, and V. N. Bringi, "Differential reflectivity and its use in the radar measurement of rainfall," Atmos. Sci. Prog., Ohio State Univ., Columbus, Rep. AS-S-106, Apr. 1979.
[12] R. List, and J. R. Gillespie, "Evolution of raindrop spectra with collision-induced breakup," *J. Atmos. Sci.*, vol. 33, pp. 2007–2013, 1976.
[13] A. Waldvogel, "The N_0 jump of raindrop spectra," *J. Atmos. Sc.*, vol. 31, pp. 1067–1077, 1974.
[14] E. A. Mueller, and E. J. Silha, "Unique features of the CHILL radar," in *Proc. 18th AMS Conf. Radar Meteorology*, Mar. 28–31, 1978, Atlanta, GA, pp. 381–382, 1978.

A Model for the Microwave Emissivity of the Ocean's Surface as a Function of Wind Speed

THOMAS T. WILHEIT, JR., SENIOR MEMBER, IEEE

Abstract—A quantitative model is presented, which describes the ocean surface as an ensemble of flat facets with a normal distribution of slopes. The variance of the slope distribution is linearly related to frequency up to 35 GHz and constant at higher frequencies. These facets are partially covered with an absorbing nonpolarized foam layer. Experimental evidence is presented for this model.

I. INTRODUCTION

THE scanning multichannel microwave radiometer (SMMR) is a five-frequency (6.6, 10.7, 18, 21, and 37 GHz) dual-polarized microwave radiometer which was carried aboard the Nimbus-7 and Seasat satellites, both of which were launched in 1978. The instrument has an 80-cm parabolic dish antenna, which scans its main beam 50° in azimuth along a conical surface with a 42°C cone angle and a vertical axis. This provides a constant incidence angle of approximately 50° at the earth's surface for the orbital altitudes of the two spacecraft (ca. 600 km Seasat, 800 km Nimbus). The spatial resolution is proportional to wavelength and varies from approximately 150 km at 6.6 GHz to 25 km at 37 GHz. The instrument has been described in detail by Gloersen and Barath [1]. The purpose of this instrument is to measure sea surface temperature and wind speed at the sea surface globally, even in the presence of clouds and light rain.

The SMMR, being a radiometer, measures the upwelling thermal microwave radiation, the intensity of which is characterized by a brightness temperature. The physical significance

Manuscript received May 2, 1979; revised August 30, 1979.
The author is with Goddard Space Flight Center, Greenbelt, MD 20771.

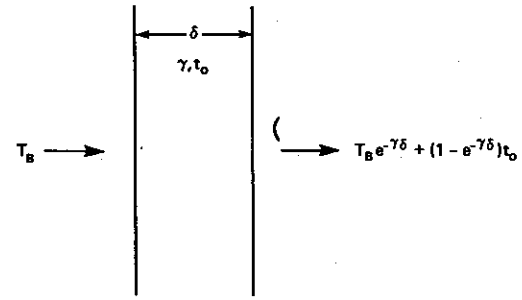

Fig. 1. The effect of an absorbing layer on a microwave radiance expressed as a brightness temperature, where T_B is the brightness temperature, γ, δ, and t_0, the absorption coefficient, thickness, and thermodynamic temperature of the layer, respectively.

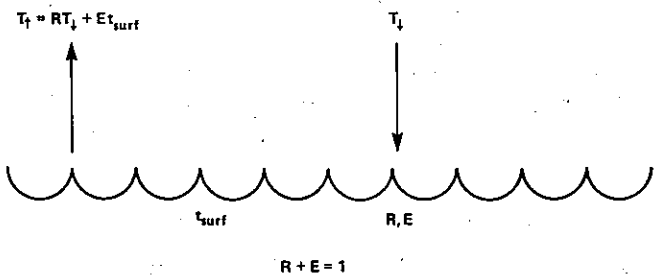

Fig. 2. The effect of reflection of a microwave radiance expressed as a brightness of a surface such as the ocean, where $T_\downarrow$ is the downwelling brightness temperature, $T\uparrow$ the upwelling brightness temperature, and E, R, and t_{surf}, the emissivity, reflectivity, and thermodynamic temperatures of the surface, respectively.

of a brightness temperature is illustrated in Fig. 1. If microwave radiation with an intensity characterized by T_B is incident on an absorbing (but not scattering or reflecting) layer with an absolute thermodynamic temperature t_0, an absorption coefficient γ, and a thickness δ, the intensity leaving the layer is given by

$$T_B' = T_B e^{-\gamma\delta} + t_0(1 - e^{-\gamma\delta}). \tag{1}$$

That is, T_B' is composed of a term representing the attenuation of the incident radiation and a complementary radiation term proportional to the absolute temperature of the absorber (Rayleigh-Jeans approximation). Note that if $T_B = t_0$, the intensity of the radiation is unchanged; the radiation is in equilibrium with the absorber. The layer in question could be a section of waveguide, an antenna, a radome, or a substantially uniform portion of the atmosphere. For computation purposes, the atmosphere is typically treated as many such layers.

A similar relationship holds for reflection at a surface as illustrated in Fig. 2. If the downwelling radiation is given by $T_\downarrow$, then the radiation upwelling off the surface $T_\uparrow$ is given by

$$T_\uparrow = RT_\downarrow + Et_s \tag{2}$$

where R is the power reflectivity of the surface, E is the emissivity of the surface, and t_s is the absolute thermodynamic temperature of the surface. Consideration of thermodynamic equilibrium requires that

$$R + E = 1. \tag{3}$$

The absorption properties of the atmosphere have been discussed by Chang and Wilheit [2]. The dominant features in the frequency range of interest here are a weak water vapor resonance centered at 22.235 GHz and absorption due to nonraining clouds which is approximately proportional to the square of the frequency. The entire problem of radiative transfer in the presence of rain is much more complicated because scattering as well as absorption must be considered [3].

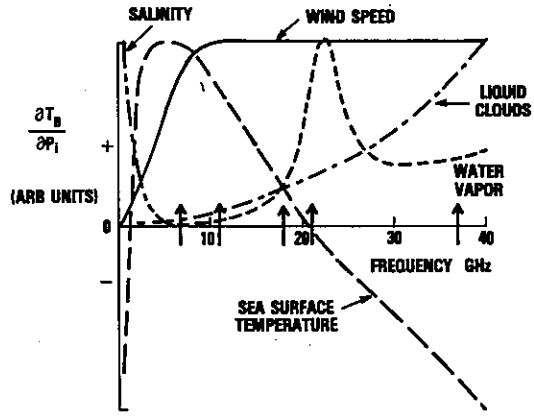

Fig. 3. Schematic superposition of the spectra of various geophysical parameters, P_i. The arrows indicate the SMMR frequencies; the signs have been chosen to be positive and the frequency range of primary importance to the given parameter.

Fig. 3 is a schematic superposition of the spectra of all the parameters of interest here including the reflection and emission properties of the ocean's surface which are the subject of this paper. The ordinate is the partial derivative of the upwelling brightness temperature with respect to the parameter of interest $\partial T_B/\partial P_i$, expressed in arbitrary units. The polarity has been chosen to make the effect positive where it is important. The frequencies of the SMMR are marked with the arrows. One can see that these are well-chosen frequencies for sorting out these effects. There is also some information content in the polarization of the brightness temperatures but that is not so easily displayed; it is, however, implicitly exploited in schemes to retrieve the various parameters from the brightness temperature measurements [2], [4]-[6]. Simulations based on these retrieval schemes and measured performance of the SMMR instrument [4]-[6] indicate that an rms measurement accuracy of 1.5°C is attainable for the sea surface temperature. The lowest frequency, 6.6 GHz, is used in this retrieval thus the spatial resolution is limited to roughly 150 km. Similarly, the surface wind speed can be extracted from the measurements to roughly 1 m/s accuracy. The lowest frequency used for estimating surface wind speed is 10.7 GHz, so approximately 90-km spatial resolution is attained. Atmospheric water can be retrieved with a spatial resolution of 60 km and an accuracy of 0.15 g/cm^2 and 4 mg/cm^2 for the vapor and liquid phases, respectively.

In the various discussions [2], [4]-[6] of the retrieval schemes, it is obvious that the major uncertainty in the required modeling is the effect of the wind on the microwave emissivity of the ocean's surface. All the other elements of the modeling are based on laboratory measurements and well-established applications of the theory of electromagnetic radiation. The purpose of this paper is to document the model used in the version of the retrieval algorithm [6] used at

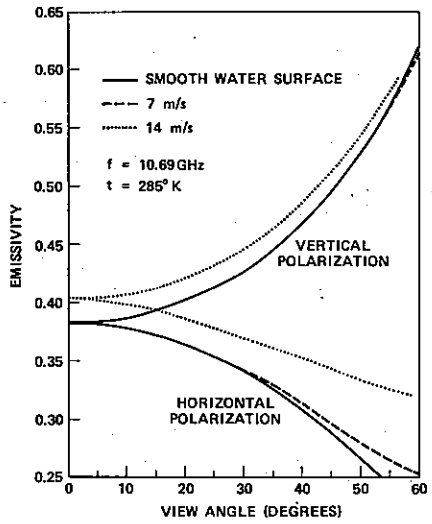

Fig. 4. Emissivity as a function of view angle for a smooth water surface and for the ocean surface with 7- and 14-m/s wind speed.

launch of the two spacecraft, to justify the use of this, and to examine its limitations. For sake of readability, the model will be presented first without justification and then compared with observations.

II. The Model

It is a straightforward problem to calculate the emissivity of a smooth water surface. The dielectric properties of sea water and saline solutions have been discussed by many authors [7]-[9]. We will use values derived from the Lane and Saxton [7] measurements and expressed in an analytic form by Chang and Wilheit [2]. The formalism for calculating the emissivity for a given view angle and polarization is the so-called Fresnel relations [10]. The resulting emissivity as a function of view angle is shown in Fig. 4 for a frequency of 10.7 GHz and a temperature of 285 K. This smooth surface model was also used for calculating the surface temperature and salinity sensitivity curves shown in Fig. 3. They were calculated for a view angle of 50° and vertical polarization; the results are similar for other angles and for horizontal polarization.

However, the ocean's surface is not a smooth surface; the wind roughens the surface, and if it is blowing hard enough, partially covers the surface with foam. It is necessary at this point to define more precisely what is meant by surface wind speed. The wind varies with height near the surface and the details of this variation depend on the temperature difference between the air and the sea [11]. When the air is warmer than the ocean (stable), there is more wind shear than for the opposite (unstable) case for a given wind speed at some reference level. The wind for our purpose is measured near the surface ($\lesssim$ 200 m) along with the air and sea temperatures. These data are then used to calculate the so-called friction velocity U^* at the sea surface by means of the Cardone [11] model. U^* is then related to wind at 20-m height, assuming that the sea and air temperature are equal (neutral stability). This last step is simply a one-for-one transformation to express the friction velocity in more familiar terms. Wherever possible in this paper, the winds have been converted to this 20-m neutral stability wind.

Cox and Munk [12] have quantitatively described the distribution of surface slopes as a function of wind speed. They found that the surface slopes were normally distributed with a variance, given by

$$\sigma_{cm}^2 = 0.003 + .0048W \tag{4}$$

where W is the wind speed in meters/seconds at 20-m height. The factor multiplying W in the above equation is slightly different from that in the Cox and Munk [12] paper because the winds were measured at 12.5 m in their work. These measurements were made at visible wavelengths. Much of the roughness they observed is at scales very small compared to microwave wavelengths. The model presented here requires only a fraction of the Cox and Munk roughness at the longer microwave wavelengths similar to an observation by Hollinger [16]. Specifically, the slope variance observed at a given microwave frequency is

$$\sigma^2(f) = (0.3 + 0.02f(\text{GHz}))\sigma_{cm}^2, \quad f < 35 \text{ GHz}$$
$$\sigma^2(f) = \sigma_{cm}^2, \quad f \geq 35 \text{ GHz}. \tag{5}$$

To calculate a rough surface emissivity from this slope distribution, one simply averages the Fresnel relations [10] over the distribution of surface slopes, taking care to treat polarization properly and to account for the projection of the facet in the view direction. In doing so, one implicitly ignores surface curvature and all structure comparable to a wavelength and thereby reduces the problem to geometric optics. This is similar to the Stogryn [13] calculation but derived in a simpler manner by making physical approximation before getting into the mathematics of the problem. The comparison with observations which follow will demonstrate that this is a surprisingly good approximation.

Wind also creates foam on the ocean's surface. Nordberg *et al.* [14] found a linear increase in brightness temperature with wind speed whenever the wind speed exceeded 7 m/s. They were viewing directly at the nadir, which essentially eliminates the roughness effect, leaving foam as the most reasonable explanation. In our model, we will treat foam as partially obscuring the surface in a manner independent of polarization. A nonreflecting material partially covering the surface would have this property as would an absorbing but partially transparent medium with the same temperature as the water. Either description alone would be inadequate, but a combination of the two descriptions would be closer to reality. The degree to which foam obscures the surface is frequency dependent and proportional to the amount by which the wind speed exceeds 7 m/s. A reasonable approximation to the available observations [17], [18] of the fraction K, by which the surface reflectivity is reduced by foam, is

$$K \cong a(1 - e^{-f/f_0})(w - 7 \text{ m/s}), \quad w \geq 7 \text{ m/s}$$
$$K = 0, \quad w < 7 \text{ m/s} \tag{6}$$

where f is the frequency, $a = 0.006$ s/m, and $f_0 = 7.5$ GHz.

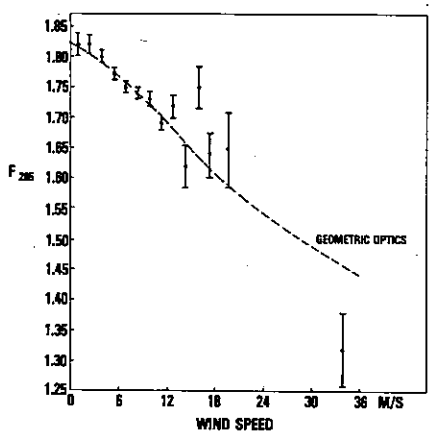

Fig. 5. Observed value of $F_{285} = (T_H - 285)/T_V - 285)$ and wind speeds. The geometric optics curve is based on the Cox and Munk [12] distribution of the surface slopes [15].

Emissivities calculated according to this model for 7 and 14 m/s are shown in Fig. 4 for comparison with the emissivity of a smooth surface.

III. Supporting Observations

Because the assumed foam model has no polarization character, dual-polarized observations of the surface provide a test of the rough surface portion of the model. If one makes the approximation that the atmosphere and the surface have the same thermodynamic temperature T_1, then it is straightforward to show that for any given view angle:

$$F_{T_1}(\theta) = \frac{T_H(\theta) - T_1}{T_V(\theta) - T_1} = \frac{R_H(\theta)}{R_V(\theta)}. \tag{7}$$

Here $T_H(\theta)$ is the horizontal brightness temperature at an angle θ and $R_H(\theta)$ is the horizontally polarized reflectivity. $T_V(\theta)$ and $R_V(\theta)$ refer similarly to vertical polarization. Note that because $F_{T_1}(\theta)$ is the ratio of two reflectivities, it is independent of foam cover and thus provides a measurement of surface roughening. The data from the electrically scanned microwave radiometer (ESMR) on Nimbus-6 (37 GHz, 50° view angle) have been so analyzed and compared with wind speeds derived from the operational data buoys [15]. A summary of this comparison is given in Fig. 5. The plotted data are for the most part, averages of many observations; a total of 264 observations are represented. In analyzing the data, it was found that a value of 285 K for T_1 worked best, but that the improvement over any value in the range 280 K–290 K was only marginal. Using the model described in the previous section, the expected value of F_{285} has been calculated: the agreement with the observations is striking. A geometric optics model using the Cox and Munk sea surface slope distribution works extremely well at a wavelength of 0.8 cm and a view angle of 50°, Hollinger [16] has made observations from a fixed platform at frequencies of 1.4, 8.36, and 19.34 GHz. He has filtered the data to remove most of the foam effect, but application of an analysis technique similar to that applied to the Nimbus-6 ESMR data certainly removes the remainder. These data can be interpreted in terms of the geometric optics model but with much less slope variance than the Cox and Munk [12] values.

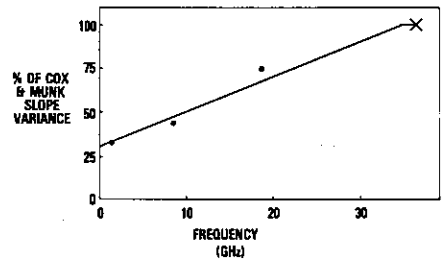

Fig. 6. Percentage of Cox and Munk [12] slope variance required for a geometric optics model to explain the Nimbus-7 observations [15] (X) and Hollinger [16] (·) as a function of frequency.

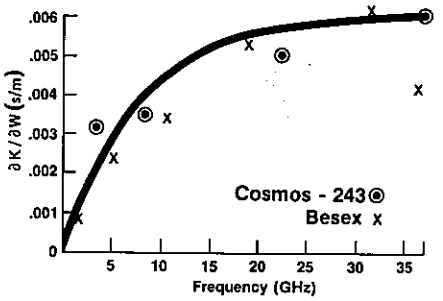

Fig. 7. Frequency dependence of the extent to which wind-induced foam increases the microwave emissivity of the ocean surface.

The fraction of the Cox and Munk slope variance required to account for the Hollinger [16] data at 55° incidence angle are plotted in Fig. 6. The Hollinger data are consistent with these roughness fractions for all view angles between 0 and 55°. The Nimbus-6 ESMR [15] result is also shown in Fig. 6. These data form a picture consistent with the roughness required in (5) (shown as a solid line).

The data of Cox and Munk [12] also suggested some anisotropy. That is, they found somewhat different upwind, downwind, and crosswind slope distributions. In the analysis of the Nimbus-6 ESMR data [15], a search was made for this anisotropy and it was not found in the microwave data. It was determined that the upper limit for anisotropy in the roughening was equivalent to 2 m/s wind. We have, therefore, used the isotropic approximation also presented by Cox and Munk [12].

The primary available observations relevant to the effect of foam on surface emissivity are from the Bering Sea expedition (BESEX) [17] and from Cosmos 243 [18]. These results along with a plot of $\partial K/\partial W$ are given in Fig. 7. The observations are difficult but nevertheless show reasonable self-consistency except possibly for the one BESEX point at 37 GHz.

IV. Limitations of the Model

There are two obvious limitations to this model, the lack of physical optics effects and the simplistic treatment of foam. If one calculates the nadir emissivity of the surface according to the present geometric-optics model there is substantially no change in emissivity through the entire 0–7 m/s wind speed range. Blume *et al.* [18] have published the observations in

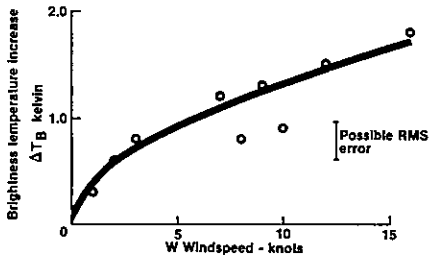

Fig. 8. Brightness temperature increase due to wind speed at 2.65 GHz from Blume *et al.* [19].

Fig. 8. These observations at 2.65 GHz show a brightness temperature increase with increasing wind speed of approximately 0.2 K/m/s which corresponds to an apparent emissivity increase of 7×10^{-3} s/m. Even if one allows for the finite antenna beamwidth (20.5°) and the increasing contribution of reflected sky emission with increasing wind-induced roughness, only about a quarter of this effect can be accounted for. There were not sufficient data in the paper [18] to permit detailed calculations of the reflected solar radiation. However, this factor is estimated to be the correct magnitude to account for much of the observed effect. In any case, these observations suggest an upper limit to the physical optics contribution of about 5×10^{-3} s/m.

The treatment of foam as having neither polarization properties nor view angle dependence is clearly too simple. Williams [20] has investigated the properties of gelatin-stabilized bubble rafts under laboratory conditions. His results suggest that the increase of emissivity caused by foam is caused by the distortion of the meniscus at the foam-water interface which provides a gradual transition from the dielectric constant of air to that of water. His results with bubble rafts on an aluminum surface suggest that in the bulk of the foam the imaginary part of the index of refraction is on the order of 1 percent that of water. His results form the basis of a calculation of foam emissivity to be used as a credibility check on our foam description. Specifically, we assume a 1-cm thick layer with a complex index of refraction.

$$n_{\text{foam}} = ((n_{\text{water}} - 1)/100.) + 1 \tag{8}$$

where n_{water} is the complex index of refraction of water, to represent the bulk of the foam and a linear transition from n_{foam} to n_{water} to represent the meniscus. The thickness of this linear transition (0.6 cm) was adjusted to provide a reasonable fit to the value of f_0 used in (6). This differs from the model of Droppelman [21] in that he used only the constant index of refraction layer and no transition region. The emissivity was calculated [20] as a function of frequency and view angle. The foam-coverage efficiency E_F was defined in terms of the horizontally polarized emissivity of the foam E_H^{foam} and of smooth water E_H^{water}.

$$E_F \equiv \frac{E_H^{\text{foam}} - E_H^{\text{water}}}{1 - E_H^{\text{water}}}. \tag{9}$$

Foam-coverage efficiencies so calculated are shown in Fig. 9 for view angles of 5° and 55°. The foam-coverage efficiency implied in (6), $(1 - e^{-f/f_0})$, is shown for comparison. Except for some structure which is an artifact of the calculation, (resonances within the 1-cm foam layer) and which certainly would not be observed in natural foam, the agreement is

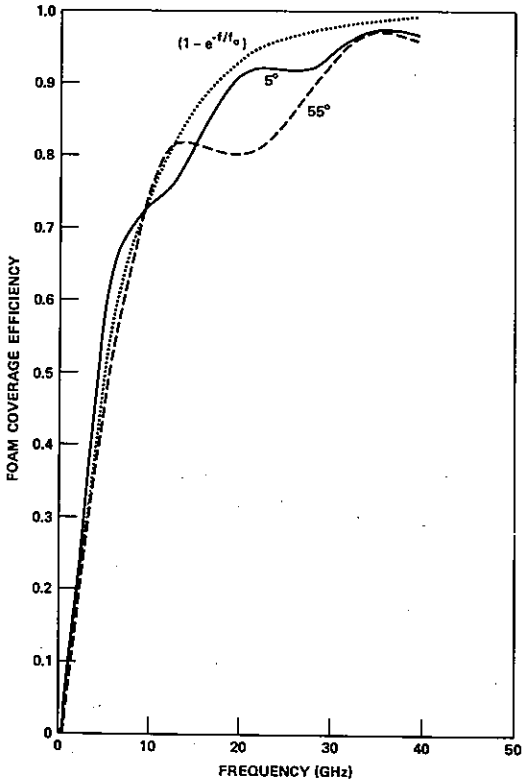

Fig. 9. Foam-coverage efficiency calculated with a 6-mm linear index of refraction transition and a 1-cm weakly absorbing layer.

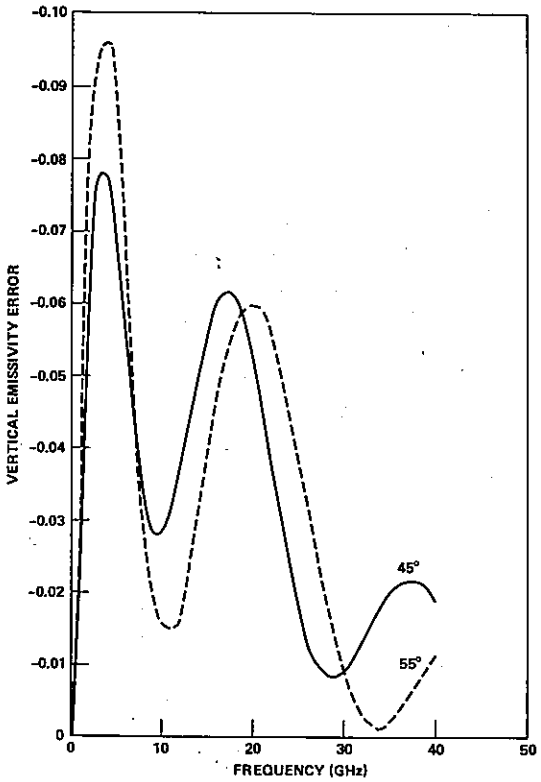

Fig. 10. Approximate error in vertical emissivity at 100-percent foam cover due to ignoring polarization properties of foam.

reasonable suggesting that ignoring view angle effects in our description of foam may not be too serious.

The lack of polarization character in the foam is more serious. By assuming that foam partially obscures the surface, the horizontal and vertical reflectivities are reduced in the same proportion, i.e.,

$$1 - E_V^{\text{foam}} = \frac{(1 - E_H^{\text{foam}})(1 - E_V^{\text{water}})}{(1 - E_H^{\text{water}})}. \quad (10)$$

In Fig. 10, the vertical emissivity error made in this assumption is shown for view angles of 45° and 55°. The error is less for smaller angles and vanishes identically for 0°. The resonances observed in Fig. 9 are observed in Fig. 10 and must be similarly discounted. Nevertheless errors of about 0.05 in the vertical emissivity would be expected even for 100-percent foam cover (wind speed greater than 170 m/s). The sign of the error is such that the true emissivity in vertical polarization is somewhat greater than (10) would suggest.

V. Conclusion

A model has been presented for the microwave emissivity of a wind-roughened foam-covered ocean. The roughness portion of the description is remarkably consistent with observations; the foam effects show somewhat more scatter. The strength of the foam-cover effect at 6.6 and 10.7 GHz are important parameters in the interpretation of Nimbus-7 and Seasat SMMR data; the strength at higher frequencies less so. In comparing the space observations with surface measurements of temperature and wind speed, it should be possible to adjust the foam effect at these two frequencies in order to refine the retrieval algorithm.

References

[1] P. Gloersen and F. T. Barath, "A scanning multichannel microwave radiometer for Nimbus-G and Seasat-A," *IEEE Trans. Oceanic Eng.*, vol. OE-2, pp. 172–178, 1977.

[2] A. T. C. Chang and T. T. Wilheit, "Remote sensing of atmospheric water vapor, liquid water, and wind speed at the ocean surface by passive microwave techniques from the Nimbus-5 satellite," NASA TM-79568, June 1978, to be published in *Radio Sci.*

[3] T. T. Wilheit, A. T. C. Chang, M. S. V. Rao, E. B. Rodgers, and J. S. Theon, "A satellite technique for quantitatively mapping rainfall rates over the oceans," *J. Appl. Meteorol.*, vol. 16, pp. 551–650, 1977.

[4] T. T. Wilheit, "A review of applications of microwave radiometry to ocenaography," *Bdy. Layer Met.*, vol. 13, pp. 277–293, 1978.

[5] T. T. Wilheit, A. T. C. Chang, and A. S. Milman, "Atmospheric corrections to passive microwave observations of the ocean," Invited paper presented at the Inter Union Commission on Radio Meteorology Colloquium on Passive Radiometry of the Ocean's Surface, Patricia Bay, B. C., Canada, 1978, to be published in *Bdy. Layer Met.*

[6] T. T. Wilheit and A. T. C. Chang, "An algorithm for the retrieval of surface and atmospheric parameters from the observations of the scanning multichannel microwave radiometer (SMMR) over oceans," NASA TM-80277, 1979, submitted to *Radio Sci.*

[7] J. A. Lane and J. A. Saxton, "Dielectric disperson in pure polar liquids at very high radio frequencies," in *Proc. Roy. Soc.*, London A, vol. 214, pp. 531–545, 1952.

[8] L. A. Kline and C. T. Swift, "An improved model for the dielectric constant of sea water at microwave frequencies," *IEEE Trans. Antennas Propagat.*, vol. AP-25, pp. 104–111, 1977.

[9] A. Strogryn, "Equations for calculating the dielectric constant of saline water," *IEEE Trans. Microwave Theory Tech.*, MTT-19, pp. 733–736, 1971.

[10] J. D. Jackson, *Classical Electrodynamics.* New York: Wiley, 1962, p. 216ff.

[11] V. J. Cardone, "Specification of the wind distribution in the marine boundary layer for wave forecasting," Ph.D. dissertation, New York Univ., Dep. Meteorol. and Oceanography, 1969. (Available from NTIS order no. AD702490.)

[12] C. Cox and W. Munk, "Some problems in optical oceanography," *J. Marine Res.*, vol. 4, pp. 63–78, 1955.

[13] W. Nordberg, J. Conaway, D. B. Ross, and T. Wilheit, "Measurements of microwave emission from a foam-covered wind driven sea," *J. Atmos. Sci.*, vol. 38, pp. 429–433, 1971.

[14] A. Strogryn, "The apparent temperature of the sea at microwave frequencies," *IEEE Trans. Antennas Propagat.*, vol. AP-15, pp. 278–286, 1967.

[15] T. T. Wilheit, "The effect of wind on the microwave emission from the ocean's surface at 37 GHz," NASA TM-79588, July 1978, to be published in *J. Geophys. Res.*

[16] J. P. Hollinger, "Passive microwave measurements of sea surface roughness," *IEEE Trans. Geosci. Electron.*, vol. GE-9, pp. 165–169, 1971.

[17] W. J. Webster, Jr., T. T. Wilheit, D. B. Ross, and P. Gloersen, "Spectral Characteristics of the microwave emission from a wind driven foam-covered sea," *J. Geophys. Res.*, vol. 81, pp. 3095–3099, 1976.

[18] A. Shutko, "Report on Soviet progress in microwave radiometry of the ocean's surface," presented at the IUCRM Colloquium on Passive Radiometry of the Ocean's Surface, Patricia Bay, B. C., Canada, June 1978.

[19] H-J. C. Blume, A. W. Love, M. J. Van Melle, and W. W. Ho, "Radiometric observations of sea temperature at 2.65 GHz over the Chesapeake Bay," *IEEE Trans. Antennas Propagat.*, vol. AP-25, pp. 121–128, 1977.

[20] G. F. Williams, "Microwave emissivity measurements of bubbles and foam," *IEEE Trans. Geosci. Electron.*, vol. GE-9, pp. 221–224, 1971.

[21] J. D. Droppleman, "Apparent microwave emissivity of sea foam," *J. Geophys. Res.*, vol. 75, pp. 696–698, 1970.

[22] T. T. Wilheit, "Radiative transfer in a plane stratified dielectric," *IEEE Trans. Geosci. Electron.*, vol. 16, pp. 138–143, 1978.